

Determination of the pion charge form factor for $Q^2=0.60-1.60$ (GeV/c)²

V. Tadevosyan,¹ H.P. Blok,^{2,3} G.M. Huber,⁴ D. Abbott,⁵ H. Anklin,^{6,5} C. Armstrong,⁷ J. Arrington,⁸ K. Assamagan,⁹ S. Avery,⁹ O.K. Baker,^{9,5} C. Bochna,¹⁰ E.J. Brash,⁴ H. Breuer,¹¹ N. Chant,¹¹ J. Dunne,⁵ T. Eden,^{12,5} R. Ent,⁵ D. Gaskell,¹³ R. Gilman,^{14,5} K. Gustafsson,¹¹ W. Hinton,⁹ H. Jackson,⁸ M.K. Jones,⁷ C. Keppel,^{9,5} P.H. Kim,¹⁵ W. Kim,¹⁵ A. Klein,¹⁶ D. Koltenuk,¹⁷ M. Liang,⁵ G.J. Lolos,⁴ A. Lung,⁵ D.J. Mack,⁵ D. McKee,¹⁸ D. Meekins,⁷ J. Mitchell,⁵ H. Mkrtchyan,¹ B. Mueller,⁸ G. Niculescu,⁹ I. Niculescu,⁹ D. Pitz,¹⁹ D. Potterveld,⁸ L.M. Qin,¹⁶ J. Reinhold,⁸ I.K. Shin,¹⁵ S. Stepanyan,¹ L.G. Tang,^{9,5} R.L.J. van der Meer,⁴ K. Vansyoc,¹⁶ D. Van Westrum,²⁰ J. Volmer,^{2,3} W. Vulcan,⁵ S. Wood,⁵ C. Yan,⁵ W.-X. Zhao,²¹ and B. Zihlmann^{22,5}

(The Jefferson Lab F_π Collaboration)

¹Yerevan Physics Institute, 375036 Yerevan, Armenia

²Faculteit Natuur- en Sterrenkunde, Vrije Universiteit, NL-1081 HV Amsterdam, The Netherlands

³NIKHEF, Postbus 41882, NL-1009 DB Amsterdam, The Netherlands

⁴University of Regina, Regina, Saskatchewan S4S-0A2, Canada

⁵Physics Division, TJNAF, Newport News, Virginia 23606

⁶Florida International University, Miami, Florida 33119

⁷College of William and Mary, Williamsburg, Virginia 23187

⁸Argonne National Laboratory, Argonne, Illinois 60439

⁹Hampton University, Hampton, Virginia 23668

¹⁰University of Illinois, Champaign, Illinois 61801

¹¹University of Maryland, College Park, Maryland 20742

¹²Norfolk State University, Norfolk, Virginia 23504

¹³Oregon State University, Corvallis, Oregon 97331

¹⁴Rutgers University, Piscataway, New Jersey 08855

¹⁵Kyungpook National University, Taegu, Korea

¹⁶Old Dominion University, Norfolk, Virginia 23529

¹⁷University of Pennsylvania, Philadelphia, Pennsylvania 19104

¹⁸New Mexico State University, Las Cruces, New Mexico 88003-8001

¹⁹DAPNIA/SPhN, CEA/Saclay, F-91191 Gif-sur-Yvette, France

²⁰University of Colorado, Boulder, Colorado 76543

²¹M.I.T.-Laboratory for Nuclear Sciences and Department of Physics, Cambridge, Massachusetts 02139

²²University of Virginia, Charlottesville, Virginia 22901

(Dated: July 11, 2006)

The data analysis for the reaction $^1\text{H}(e, e'\pi^+)n$, which was used to determine values for the charged pion form factor F_π for values of $Q^2=0.6-1.6$ (GeV/c)², has been repeated with careful inspection of all steps and special attention to systematic uncertainties. Also the method used to extract F_π from the measured longitudinal cross section was critically reconsidered. Final values for the separated longitudinal and transverse cross sections and the extracted values of F_π are presented.

PACS numbers: 14.40.Aq, 11.55.Jy, 13.40.Gp, 25.30.Rw

Hadron form factors are an important source of information on hadronic structure. Of these, the charge form factor, F_π , of the (charged) pion plays a special role. One of the reasons is that the valence structure of the pion is relatively simple. Furthermore, in contrast to the nucleon case, the asymptotic normalization of the pion wave function, and hence the behavior of $F_\pi(Q^2)$ at large Q^2 is known from the decay of the pion.

The behavior of F_π at very low values of Q^2 has been determined up to $Q^2=0.28$ (GeV/c)² from scattering high-energy pions from atomic electrons [1]. At higher values of Q^2 the $^1\text{H}(e, e'\pi^+)n$ reaction is employed. At low values of the Mandelstam variable $|t|$ the virtual photon couples to a virtual pion in the proton. This allows F_π to be determined from the longitudinal cross section, which globally follows F_π^2 . In this way the

pion form factor was studied for Q^2 values from 0.4 to 9.8 (GeV/c)² at CEA/Cornell [2] and for $Q^2=0.35, 0.70$ (GeV/c)² at DESY [3, 4]. Ref. [4] performed a longitudinal/transverse (L/T) separation by taking data at two values of the electron energy. In the experiments done at CEA/Cornell, this was done in a few cases only, but the resulting uncertainties in σ_L were so large that the L/T separated data were not used. Consequently, the values of F_π extracted from these data have sizeable systematic uncertainties.

More recently, the $^1\text{H}(e, e'\pi^+)n$ reaction was measured at the Thomas Jefferson National Accelerator Facility (JLab) in order to study the pion form factor from $Q^2=0.6-1.6$ (GeV/c)². Because of the excellent properties of the electron beam and experimental setup at JLab,

L/T separated cross sections were determined with high accuracy. These data were used to determine the value of F_π and the results were published in Ref. [5]. Since then, the whole analysis chain has been repeated with careful investigation of all steps, including the contribution of various systematic uncertainties to the final uncertainty of the separated cross sections. Furthermore, the method to determine F_π from the longitudinal cross sections was re-investigated, leading to a different method to extract F_π . In this paper, we report on these studies and present final results for the longitudinal and transverse cross sections, as well as the extracted values of F_π . A longer paper, presenting all details of the experiment and the reanalysis will follow.

The cross section for pion electro-production can be written as

$$\frac{d^3\sigma}{dE'd\Omega_{e'}d\Omega_\pi} = \Gamma_V J(t) \frac{d^2\sigma}{dt d\phi}, \quad (1)$$

where Γ_V is the virtual photon flux factor, ϕ is the azimuthal angle of the outgoing pion with respect to the electron scattering plane, t is the Mandelstam variable $t = (p_\pi - q)^2$ and J the Jacobian for the transformation from $d\Omega_\pi$ to $dt d\phi$. The two-fold differential cross section can be written as

$$2\pi \frac{d^2\sigma}{dt d\phi} = \epsilon \frac{d\sigma_L}{dt} + \frac{d\sigma_T}{dt} + \sqrt{2\epsilon(\epsilon+1)} \frac{d\sigma_{LT}}{dt} \cos \phi + \epsilon \frac{d\sigma_{TT}}{dt} \cos 2\phi, \quad (2)$$

where ϵ is the virtual-photon polarization parameter. The cross sections $\sigma_X \equiv \frac{d\sigma_X}{dt}$ depend on W , Q^2 and t , where W is the photon-nucleon invariant mass. By using the ϕ acceptance of the experiment and taking data for the same (central) kinematics (W, Q^2, t) at two energies, and thus values of ϵ , the cross sections σ_L , σ_T , σ_{LT} and σ_{TT} can all be determined. At low values of $-t$, the longitudinal cross section σ_L is dominated by the t -pole term, which contains F_π .

By using electron energies between 2.4 and 4.0 GeV impinging on a liquid hydrogen target, and detecting the scattered electron in the Short Orbit Spectrometer (SOS) and the produced pion in the High Momentum Spectrometer (HMS) of Hall C, data for the reaction $^1\text{H}(e, e'\pi^+)n$ were taken for central values of Q^2 of 0.6, 0.75, 1.0 and 1.6 (GeV/c) 2 , at a central value of $W = 1.95$ GeV.

The data analysis is an updated version of that in Ref. [5]. First, experimental yields were determined. Electrons in the SOS were identified by using the combination of a lead glass calorimeter and gas Cerenkov detector. Pion identification in the HMS was accomplished by requiring no signal in a gas Cerenkov detector and by using time of flight between two scintillator hodoscope planes. The momenta of the scattered electron and the pion at the target vertex were reconstructed from the wire chamber information of the spectrometers, correcting for energy loss in the target. From these, the values

of Q^2 , W , t , and the missing mass were reconstructed. A cut on the latter of 0.925 to 0.96 GeV was used to select the neutron exclusive final state, excluding additional pion production. Experimental yields as function of Q^2 , W , t and ϕ were then determined by subtracting aluminum target window contributions and random coincidences (varying with bin, but typically 0.6% and 1.2%, respectively) and correcting for trigger, tracking and particle-identification efficiencies, pion absorption, local target-density reduction due to beam heating, and dead times. Details of these procedures are similar to those found in Ref. [6].

Cross sections were obtained from the yields using a detailed Monte Carlo (MC) simulation of the experiment, which included the magnets, apertures, detector geometries, realistic wire chamber resolutions, multiple scattering in all materials, optical matrix elements to reconstruct the particle momenta at the target from the information of the wire-chambers of the spectrometers, pion decay (including misidentification of the decay muon as a pion), and internal and external radiative processes.

Calibrations with the over-determined $^1\text{H}(e, e'p)$ reaction were instrumental in various applications. The beam momentum and the spectrometer central momenta were determined absolutely to better than 0.1%, while the incident beam angle and spectrometer central angles were determined with an absolute accuracy of about 0.5 mrad. The spectrometer acceptances were checked by comparison of the data to MC simulations. Finally, the overall absolute cross section normalization was checked. The calculated yields for $e + p$ elastics agreed to better than 2% with predictions based on a parameterization of the world data [7].

In the pion production reaction, the experimental acceptances in W , Q^2 and t are correlated. By using a realistic cross section model in the MC simulation, possible errors resulting from averaging the measured yields when calculating cross sections at average values of W , Q^2 and t , can be minimized. A phenomenological cross section model was obtained (see below) by fitting the different cross sections σ_X of Eqn. (2) globally to the data as a function of Q^2 and t in the whole range of Q^2 . The dependence of the cross section on W was assumed to follow the phase space factor $(W^2 - M_p^2)^{-2}$, which is supported by previous data [4].

The experimental cross sections can then be calculated from the measured and simulated yields via the relation

$$\left(\frac{d\sigma(\overline{W}, \overline{Q}^2, t, \phi)}{dt} \right)_{\text{exp}} = \frac{\langle Y_{\text{exp}} \rangle}{\langle Y_{\text{MC}} \rangle} \left(\frac{d\sigma(\overline{W}, \overline{Q}^2, t, \phi)}{dt} \right)_{\text{MC}}. \quad (3)$$

This was done for five bins in t at each of the four Q^2 -values. Here, $\langle Y \rangle$ indicates that the yields were averaged over the W and Q^2 acceptance, \overline{W} and \overline{Q}^2 being the acceptance (of high and low ϵ together) weighted average values for that t -bin. By using these average values, possible errors due to extrapolating the MC model cross section used to outside the region of the experimental

data, is avoided.

By combining for every t -bin (and for the four values of Q^2) the ϕ -dependent cross sections measured at two values of the incoming electron energy, and thus of ϵ , the experimental values of σ_L , σ_T , σ_{LT} and σ_{TT} can be determined by fitting the ϕ and ϵ -dependence. In this fit, the leading order $\sin\theta$ ($\sin^2\theta$) of σ_{LT} (σ_{TT}), where θ is the angle between the three-momentum transfer and the direction of the outgoing pion, was taken into account.¹ Those values were then used to improve upon the model cross section used in the MC simulation. This whole procedure was iterated until the values of σ_L , σ_T , σ_{LT} , and σ_{TT} converged. The dependence of σ_L (and σ_T) on the MC input model was small (see below).

The separated cross sections σ_L and σ_T are shown in Fig. 1. They are presented as differential cross sections $d\sigma/dt$ as a function of t , at the center of the t -bin. The longitudinal cross section exhibits the expected t -pole behavior. The transverse cross section is mostly flat.

The total uncertainty in the experimental cross sections is a combination of statistical and systematic uncertainties. The systematic uncertainties include contributions that, like the statistical uncertainties, are uncorrelated between the measurements at the two ϵ values, and others that are correlated. Most of the uncorrelated ones are common to all t bins, but there is a small contribution, estimated as 0.7%, that is also uncorrelated in t . The uncorrelated uncertainties are inflated by the factor $1/(\Delta\epsilon)$ in the L/T separation, where $\Delta\epsilon$ is the difference (typically 0.3) in the photon polarization between the two measurements. All contributions to the systematic uncertainty were carefully investigated, also using the results of extensive single-arm L/T separation experiments and of $^1\text{H}(e, e'p)$ calibration reactions in Hall C [8]. The uncorrelated systematic uncertainty in the unseparated cross sections common for all t -bins was estimated to be 1.7%, while the total correlated uncertainty is 2.8 - 4.1%, depending on t . Apart from a dependence of the separated cross sections on the MC model used, which ranges from 0.2% to a maximum of 3% for one highest t -bin, the largest contributions are: the detection volume (1.5%), dependence of the extracted cross sections on the momentum and angle calibration (1%), target density (1%), pion absorption (1.5%), pion decay (1%), the simulation of radiative processes (1.5%), detector efficiency corrections (1%). The overall uncertainty is slightly smaller than used in Ref. [5].

The unseparated cross sections and thus also the values of σ_L and σ_T of the present analysis differ from those of

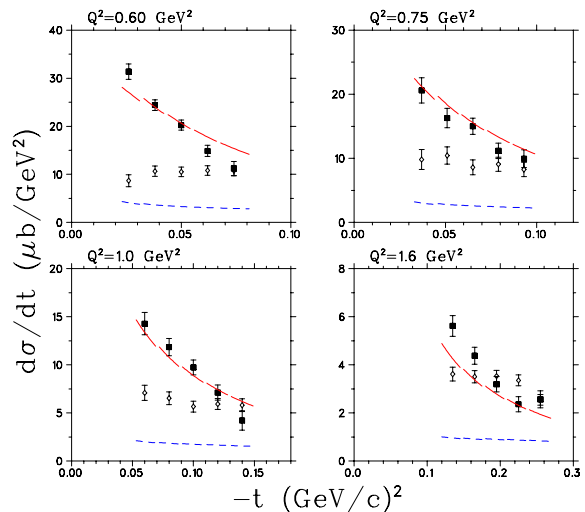


FIG. 1: Separated cross sections σ_L [solid] and σ_T [empty]. The error bars represent the combination of statistical and t uncorrelated systematic uncertainties. In addition there is an overall systematic uncertainty of about 6%, mainly from the t correlated, ϵ uncorrelated systematic uncertainty. The solid and dashed curves denote VGL model calculations for σ_L and σ_T with parameters $\Lambda_\pi^2=0.40$ (GeV/c)² and $\Lambda_\rho^2=1.5$ (GeV/c)². The discontinuities in the curves result from the different average \overline{W} and \overline{Q}^2 of each t -bin.

Ref. [5]. The new values should be considered to be more reliable, and except for a few cases, the difference is well within the total uncertainty quoted there. Compared to Ref. [5], small adjustments were made in the values of cuts and efficiencies. Also, a small mistake was found in calculating the value of θ , which affects the calculation of the cross section in Eqn. 3. Finally, the method to separate the respective cross sections was improved. On average, σ_L is 6% smaller than in Ref. [5] and σ_T is 3% larger. The greatest differences occur for $Q^2=1.0$ (GeV/c)², where σ_L is 14% smaller and σ_T is 10% larger.

Even if the t -pole process is dominant at small values of $|t|$, other processes may contribute, and the t -pole itself, as has been used in DWBA analyses of the $^1\text{H}(e, e'\pi^+)n$ reaction [4], is itself not gauge invariant. Therefore, the best way to extract F_π is to use a model that incorporates as best as possible the essential parts of the reaction. As in Ref. [5], the Regge model by Vanderhaeghen, Guidal and Laget (VGL, Ref. [9]) is used. In this model, the exchange of high-spin, high-mass particles is taken into account by replacing the pole-like Feynman propagators of Born term models with Regge propagators. Many of the model's free parameters were fitted to pion photo-production, with the result giving a good fit to existing data for $-t$ below 1 (GeV/c)². For electro-production, the pion form factor and the $\rho\pi\gamma$ form factor are included as adjustable parameters, parameterized with a monopole form $[1 + Q^2/\Lambda_\pi^2]^{-1}$. Over the range of $-t$ covered by this work, σ_L is completely determined by the π

¹ In the previous analysis [5], first σ_{LT} and σ_{TT} were determined by adjusting their values (plus a constant term) until the ratios Y_{exp}/Y_{MC} were constant as function of θ and ϕ . After that, σ_L and σ_T were determined in a Rosenbluth separation. The present method is more straightforward and has the advantage that the uncertainties in the separated cross sections are obtained more directly.

trajectory. σ_T is sensitive to the ρ exchange contribution, whose value of Λ_ρ^2 is poorly known.

The VGL model is compared to the data in Figure 1. It has been evaluated at the same \overline{W} and \overline{Q}^2 values as the data. The model strongly underestimates σ_T for any value of Λ_ρ^2 used. Since the JLab data have been taken at relatively low values of $W \approx 1.95$ GeV, this may be due to contributions from resonances, enhancing the strength in σ_T . No such terms are included explicitly in the Regge model. The VGL model calculation for σ_L gives the right magnitude, but the t dependence of the data is somewhat steeper than that of the calculations. This is most visible at $Q^2=0.6$ (GeV/c) 2 . As in the case of σ_T , the discrepancy between the data and VGL is attributed to resonance contributions. This is supported by the fact that the discrepancy is strongest at the lowest Q^2 value, at higher Q^2 the resonance form factor reduces such contributions.

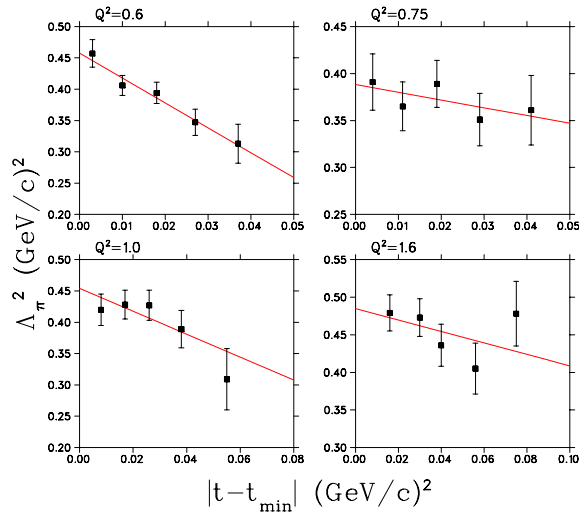


FIG. 2: Values of Λ_π^2 determined from the fit of the VGL model to each t -bin, and linear fit to same. The error bars reflect the statistical and t uncorrelated systematic uncertainties. The additional overall systematic uncertainties, which are applied after the fit, are not shown.

Since virtually nothing is known about the L/T character of resonances at $W = 1.95$ GeV and their influence on σ_L , the question is how to determine F_π . In the previous analysis [5], a lower limit for F_π was obtained by fitting Λ_π^2 at the lowest t -bin as the data are steeper than the VGL calculations. An upper limit for F_π was obtained by assuming that the ‘background’ effectively yields a negative contribution to σ_L . This background and the value of Λ_π^2 were then fitted together, assuming that the background is constant with t . Since in σ_T this ‘missing background’ (i.e. the difference between the data and VGL) decreases with decreasing $-t$, and assuming that this also holds for σ_L , this gives an upper-estimate for F_π . The best estimate for F_π was then taken as the average of the two results and one half of the average of the (relative) differences was taken as the model uncertainty.

Q^2 (GeV/c) 2	W (GeV)	Λ_π^2 (GeV/c) 2	F_π
0.60	1.95	0.458 ± 0.031	0.433 ± 0.017
0.75	1.95	0.388 ± 0.038	0.341 ± 0.022
1.00	1.95	0.454 ± 0.034	0.312 ± 0.016
1.60	1.95	0.485 ± 0.038	0.233 ± 0.014

TABLE I: Λ_π^2 and F_π values from this work. The error bars include all experimental and analysis uncertainties.

Since the publication of those results, we have looked at the discrepancy between the t -dependence predicted by the VGL model and the data in more detail by assuming, besides the VGL amplitude, a t -independent interfering background amplitude, and fitting the latter together with the value of Λ_π^2 . Although the resulting uncertainties are very large, the σ_L data weakly support an interfering amplitude whose phase is nearly orthogonal to the pion trajectory amplitude and whose magnitude decreases monotonically with increasing Q^2 . This does not necessarily result in a net negative cross section contribution to σ_L , as has been used previously. That requires a very special phase and magnitude of the interfering amplitude, which may not be realistic to assume. The assumption that the ‘background’ is independent of $-t$ is also questionable, but without this assumption the background is completely unconstrained by the data. Thus, determining F_π by fitting the interfering amplitude is not a viable method.

Given that no information is available on the background, our best estimate for F_π is determined in the following manner. Using the value of Λ_π^2 as a free parameter, the VGL model was fitted to each t -bin separately, yielding $\Lambda_\pi^2(\overline{Q}^2, \overline{W}, t)$ values as shown in Fig. 2. Λ_π^2 tends to decrease as $-t$ increases, presumably because of an interfering background. One expects the effect of the background to be smallest at the smallest value of $|t|$ allowed by the kinematics, $|t_{min}|$, so an extrapolation of Λ_π^2 to this physical limit is used to obtain our best estimate of F_π . The data at $Q^2=0.6$ and 0.75 (GeV/c) 2 suggest a linear fit versus $|t - t_{min}|$, but the data at $Q^2=1.0$ and 1.6 (GeV/c) 2 would benefit from a higher-order polynomial fit. However, since the curvature is opposite in these cases, and since one should expect the four data-sets to behave consistently, the value of Λ_π^2 at t_{min} is obtained by a linear fit in all cases. The resulting Λ_π^2 and F_π values are listed in Table I and the latter are shown in Fig. 3.

Because of the arguments given above, the values presented in Table I are our final and best estimate of F_π from these data. They are between 7 and 16% smaller than our previously published values [5], but still within the experimental and model uncertainties. The largest difference is at $Q^2 = 0.75$ (GeV/c) 2 . On average, one quarter of the difference is because the values of σ_L are smaller than those of Ref. [5], and the remaining

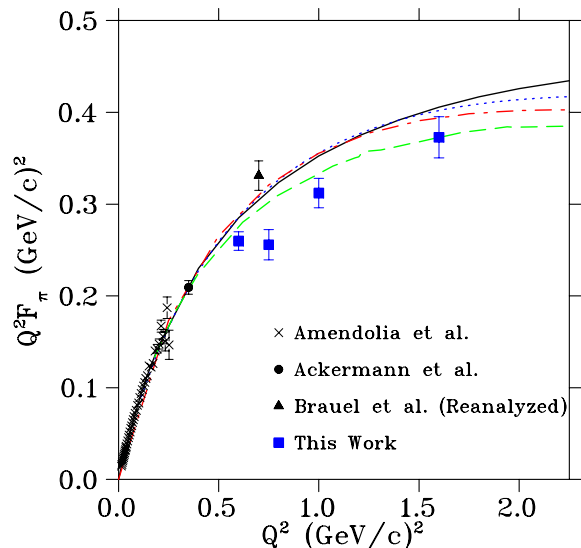


FIG. 3: $Q^2 F_\pi$ data from this work, compared to previously published data. The solid Brauel et al. [4] point has been reanalyzed using the F_π extraction method of this work. The error bars for this work and the reanalyzed Brauel et al. data include all experimental and t_{min} extrapolation uncertainties, added in quadrature. Also shown are the Dyson-Schwinger [13] (solid), QCD sum-rule [14] (dot), light front quark model [15] (dash-dot), and dispersion relation [12] (dash) calculations.

three quarters is because of the F_π extraction method, the present method being closer to the method used in Ref. [5] to get the lower limit. The data from Brauel et al. [4], taken at $Q^2=0.70$ (GeV/c) 2 and a larger value of $W=2.19$ GeV, were also reanalyzed using the present F_π extraction method. The result is 0.4% higher than that obtained using the F_π extraction method of Ref. [5]. This indicates that our F_π extraction methods are robust when the background contribution is small, as seems the case at the higher value of W . For the data presented here, the discrepancy with the t -dependence of the VGL calculation is smaller for the larger values of Q^2 and of W . This is at least compatible with the idea that resonance contributions, which presumably have a form factor that drops fast with Q^2 and get smaller at higher W ,

are responsible.

Fig. 3 compares our final data to a variety of QCD-based calculations. The data are best described by the dispersion relation calculation of Geshkenbein et al. [12]. Up to $Q^2=1.5$ (GeV/c) 2 , the Dyson-Schwinger calculation of Ref. [13], the QCD sum-rule calculation of Ref. [14] and the light front quark model calculation of Ref. [15] are nearly identical, and are all very close to the monopole form factor constrained by the measured pion charge radius [1]. The revised data are below the monopole curve, which reflects non-perturbative physics. A significant deviation would indicate the increased role of perturbative components at moderate Q^2 , while the perturbative part provides only $Q^2 F_\pi \approx 0.15-0.20$ [16].

To summarize, the data analysis for our $^1\text{H}(e, e'\pi^+)n$ experiment at $Q^2=0.6-1.6$ (GeV/c) 2 , centered at $W=1.95$ GeV, has been repeated with careful inspection of all steps. The unseparated cross sections are consistent within the uncertainty with those of our previous analysis. After the magnifying effect of the L/T separation, the resulting σ_T values are slightly larger than before, and the σ_L values are correspondingly smaller. The systematic uncertainties were critically reviewed, and are slightly smaller compared to the previous analysis. As before, we use a fit of the Regge model of Ref. [9] to our σ_L data to extract F_π . The fact that the data display a steeper t -dependence than the model is attributed to the presence of background contributions not included in the model. After revisiting our prior assumptions used to extract F_π from σ_L with the model, we employ a simpler method which relies only on the assumption that the background contributions are minimal at t_{min} , which is indicated by the data. The resulting values are our best estimate of F_π , and are between 8 and 16% smaller than before, primarily due to the different extraction method. The data indicate that for $Q^2 > 0.5$ (GeV/c) 2 , F_π starts to fall below the monopole curve that describes the low Q^2 elastic scattering data.

The authors would like to thank Drs. Guidal, Laget and Vanderhaeghen for stimulating discussions and for modifying their computer program for our needs. This work is supported by DOE and NSF (USA), FOM (Netherlands), NSERC (Canada), KOSEF (South Korea), and NATO.

-
- [1] S. R. Amendolia, *et al.*, Nucl. Phys. **B277** (1986) 168.
 - [2] C. J. Bebek, *et al.*, Phys. Rev. D **17** (1978) 1693.
 - [3] H. Ackermann, *et al.*, Nucl. Phys. **B137** (1978) 294.
 - [4] P. Brauel, *et al.*, Z. Phys. **C3** (1979) 101.
 - [5] J. Volmer, *et al.*, Phys. Rev. Lett. **86** (2001) 1713.
 - [6] J. Volmer, PhD thesis, Vrije Universiteit, Amsterdam (2000), unpublished.
 - [7] P. E. Bosted, Phys. Rev. C **51** (1995) 409.
 - [8] M.E. Christy, *et al.*, Phys. Rev. C **70** (2004) 015206.
 - [9] M. Vanderhaeghen, M. Guidal and J.-M. Laget, Phys. Rev. C **57** (1998) 1454; Nucl. Phys. **A627** (1997) 645.
 - [10] F. Gutbrod and G. Kramer, Nucl. Phys. **B49** (1972) 461.
 - [11] T. Horn, *et al.*, submitted to Phys. Rev. Lett. (2006).
 - [12] B.V. Geshkenbein, Phys. Rev. D **61** (2000) 033009.
 - [13] P. Maris, P.C. Tandy, Phys. Rev. C **62** (2000) 055204.
 - [14] V.A. Nesterenko, A.V. Radyushkin, Phys. Lett. **115 B** (1982) 410.
 - [15] C.-W. Hwang, Phys. Rev. D **64** (2001) 034011.
 - [16] A.P. Bakulev *et al.*, Phys. Rev. D **70** (2004) 033014.